Supplementary Information

Boosting Visible-light-driven Hydrogen Evolution of Covalent Organic Frameworks through Compositing with MoS_2: A Promising Candidate of Noble-Metal-Free Photocatalysts

Meng-Yao Gao,[a] Chang-Cheng Li,[a] Hong-Liang Tang,[a] Xiao-Jun Sun,*[a] Hong Dong,[a] and Feng-Ming Zhang*[a]

[a.] Key Laboratory of Green Chemical Engineering and Technology of College of Heilongjiang Province, College of Chemical and Environmental Engineering Harbin University of Science and Technology No. 4, Linyuan Road, Harbin 150040 (China).

The Turnover frequency (TOF) was calculated according to following equation:

$$\text{TON} = \frac{\text{Moles of evolved hydrogen}}{\text{Moles of } MoS_2 \text{ on photocatalyst}}$$

$$\text{TOF} = \frac{\text{TON}}{\text{reaction time (h)}}$$

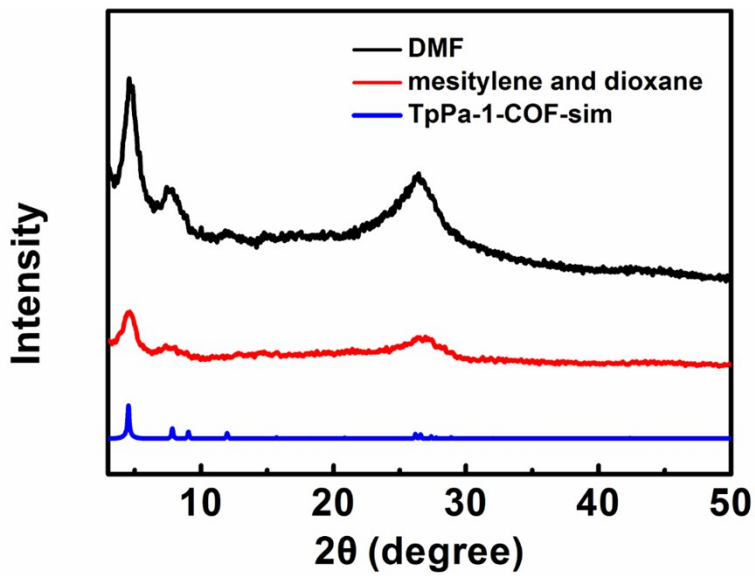

Figure S1. The XRD patterns of TpPa-1-COF in different reaction solvent.

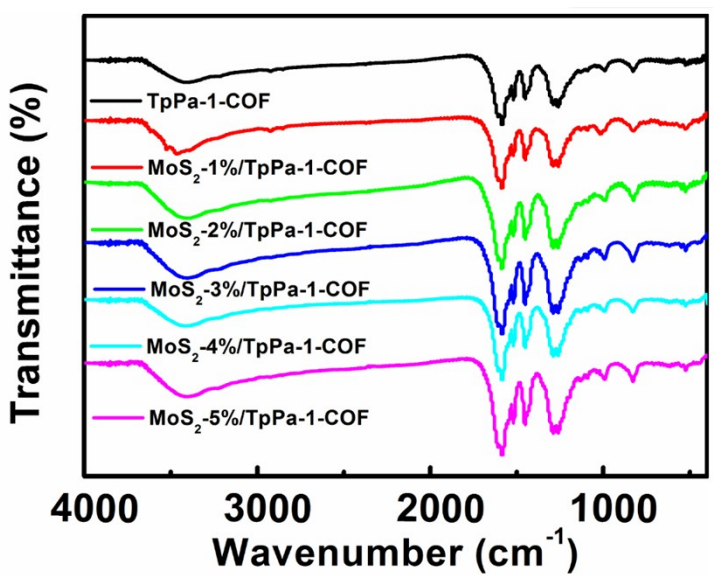

Figure S2. The FT-IR Spectra of samples with different loading amount of MoS_2 from 0 wt% to 5 wt%.

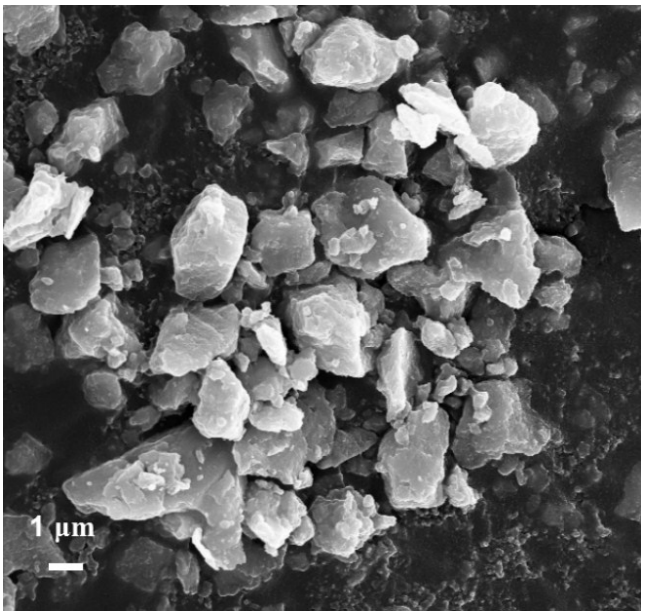

Figure S3. SEM image of bulk MoS_2.

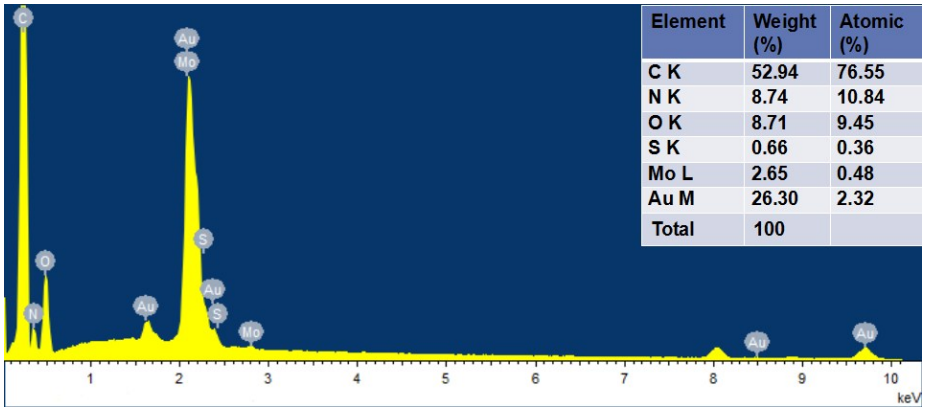

Element	Weight (%)	Atomic (%)
C K	52.94	76.55
N K	8.74	10.84
O K	8.71	9.45
S K	0.66	0.36
Mo L	2.65	0.48
Au M	26.30	2.32
Total	100	

Figure S4. EDS spectra of MoS_2-3%/TpP-1-COF.

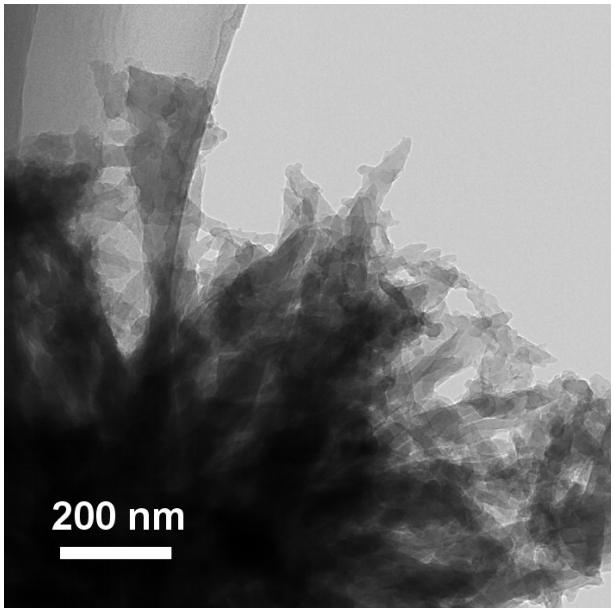

Figure S5. TEM image of TpPa-1-COF.

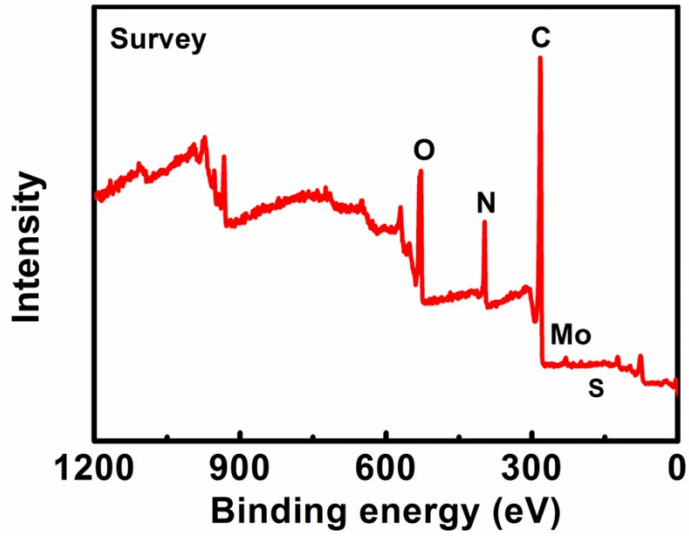

Figure S6. XPS survey spectrum of MoS_2-3%/TpPa-1-COF.

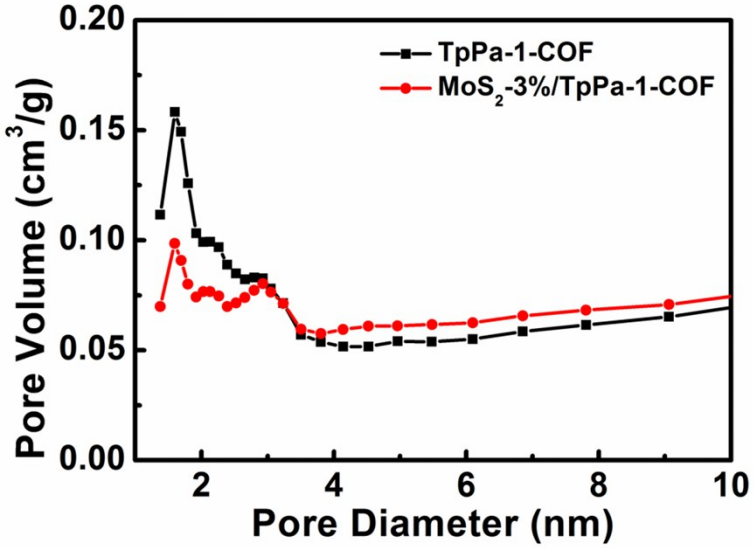

Figure S7. The pore size distribution curves for TpPa-1-COF and MoS_2-3%/TpPa-1-COF.

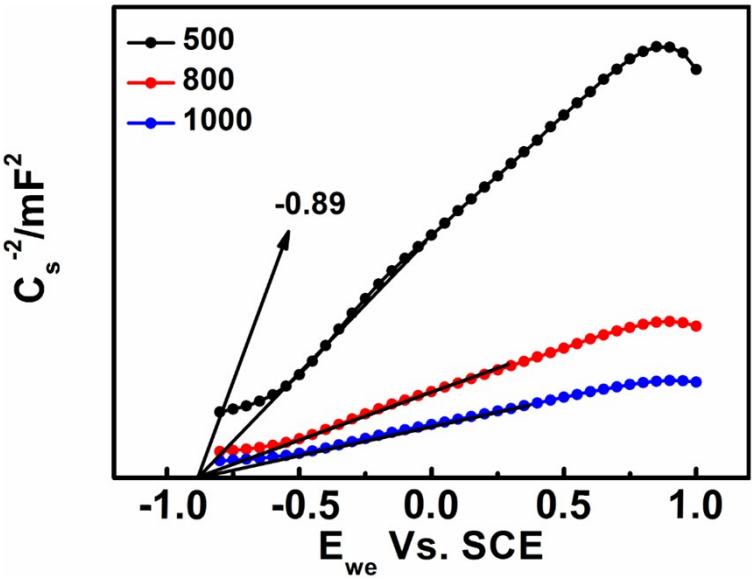

Figure S8. Mott-Schottky plots of TpPa-1-COF at three different frequencies.

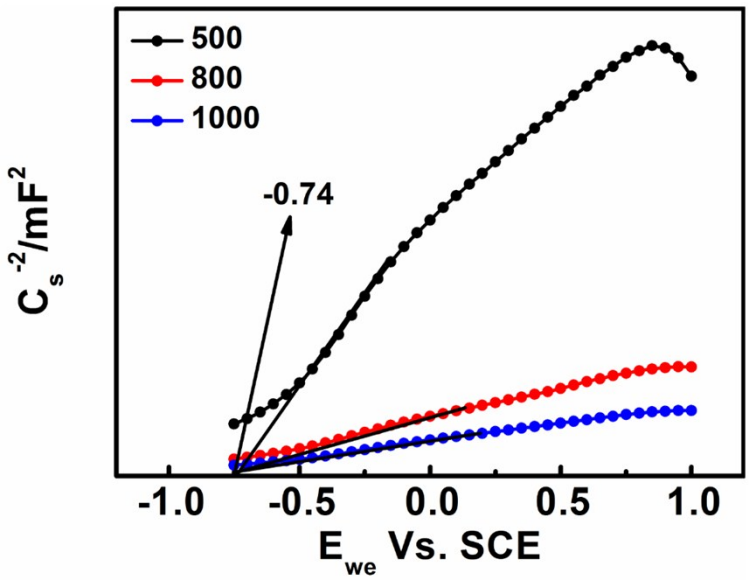

Figure S9. Mott-Schottky plots of MoS_2-3%/TpPa-1-COF at three different frequencies.

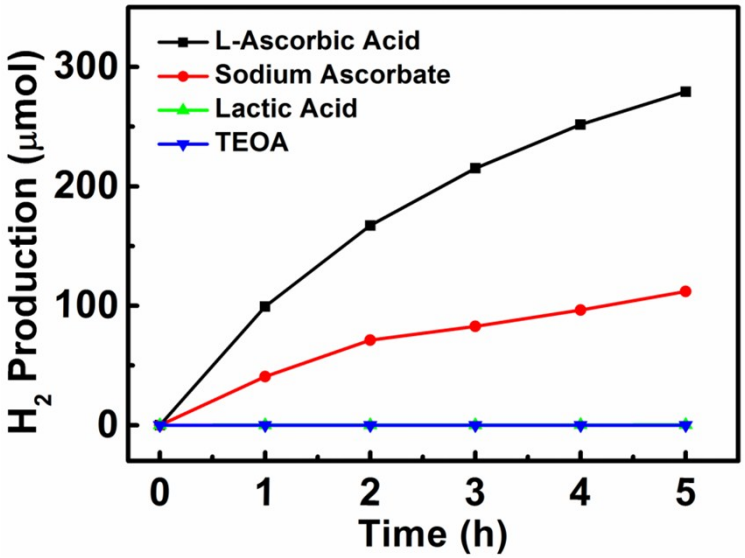

Figure S10. Comparison of the photocatalytic hydrogen evolution of MoS_2-3%/TpPa-1-COF under different sacrificial systems.

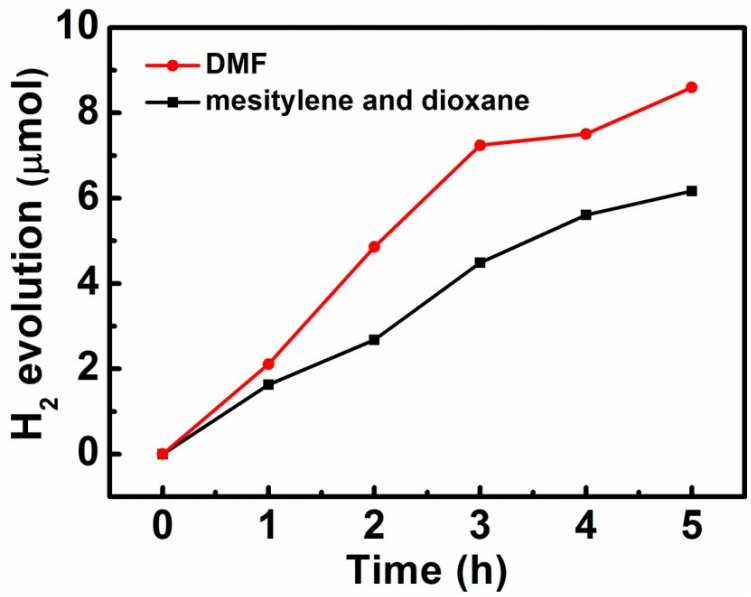

Figure S11. Comparison of the photocatalytic hydrogen evolution of TpPa-1-COF in different reaction solvent.

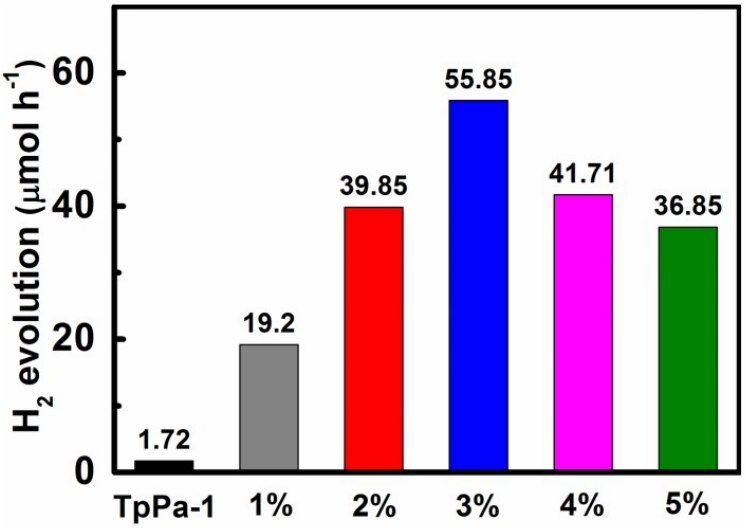

Figure S12. Average photocatalytic H_2 evolution rate of TpPa-1-COF and MoS_2/TpPa-1-COF photocatalysts with varying MoS_2 loading.

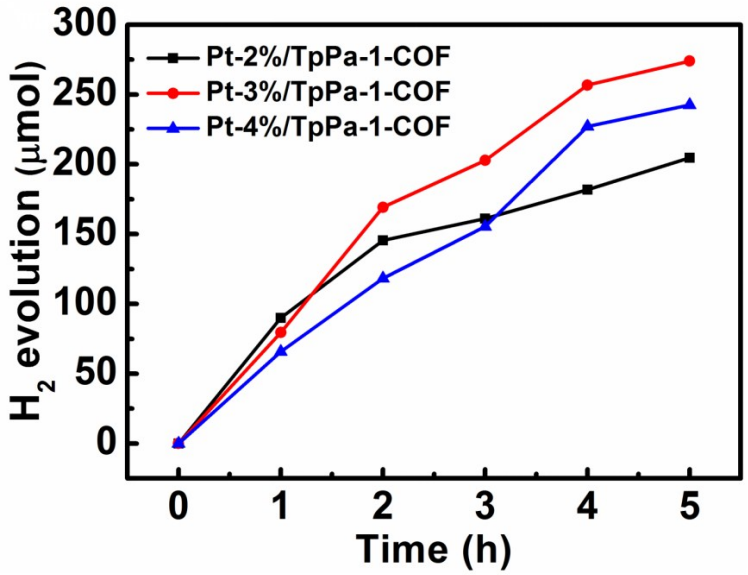

Figure S13. Photocatalytic H_2 evolution rates for TpPa-1-COF with varying amounts (2 wt%, 3 wt% and 4 wt%) of Pt as cocatalyst.

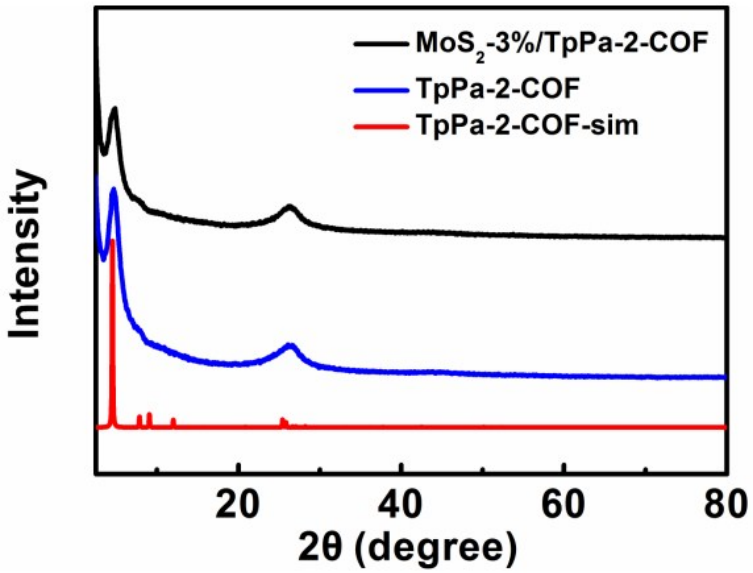

Figure S14. The XRD patterns of TpPa-2-COF and MoS_2-3%/TpPa-2-COF.

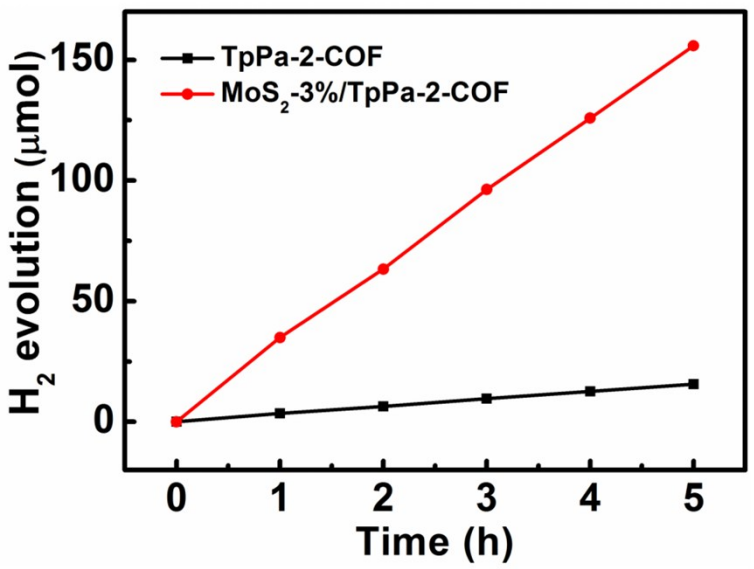

Figure S15. Photocatalytic H_2 evolution rates for TpPa-2-COF and MoS_2-3%/TpPa-2-COF.

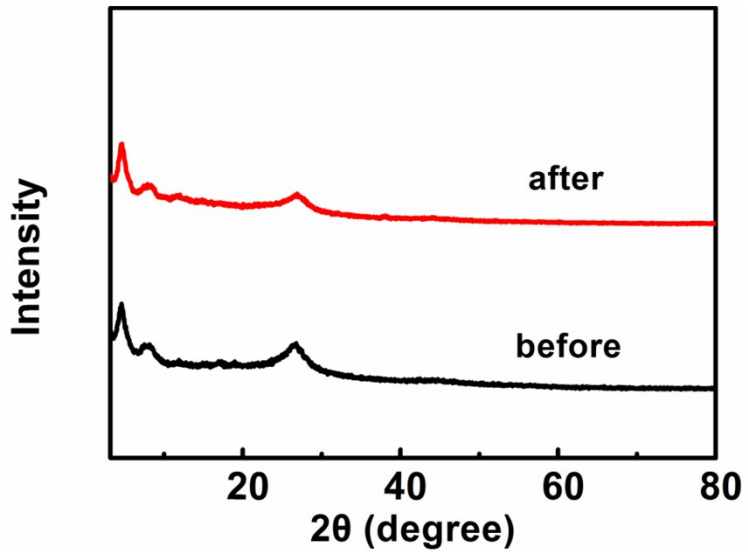

Figure S16. The XRD patterns of MoS_2-3%/TpPa-1-COF composite before and after photocatalytic reaction.

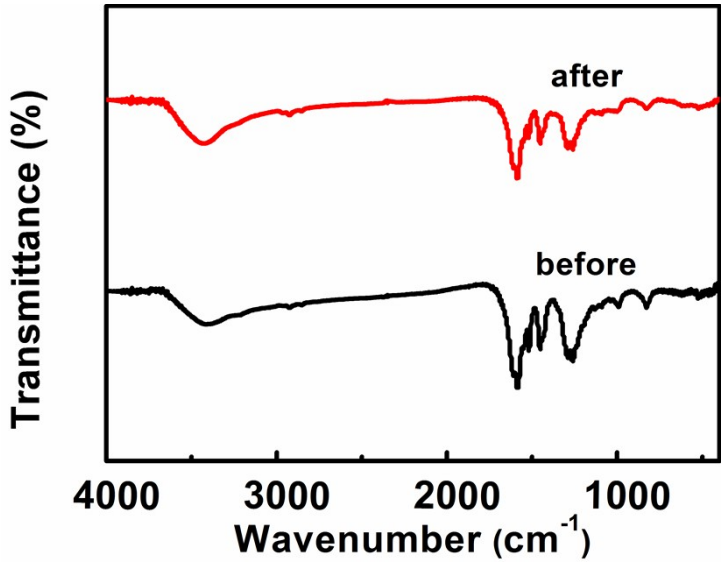

Figure S17. The IR spectrum of MoS_2-3%/TpPa-1-COF composite before and after photocatalytic reaction.

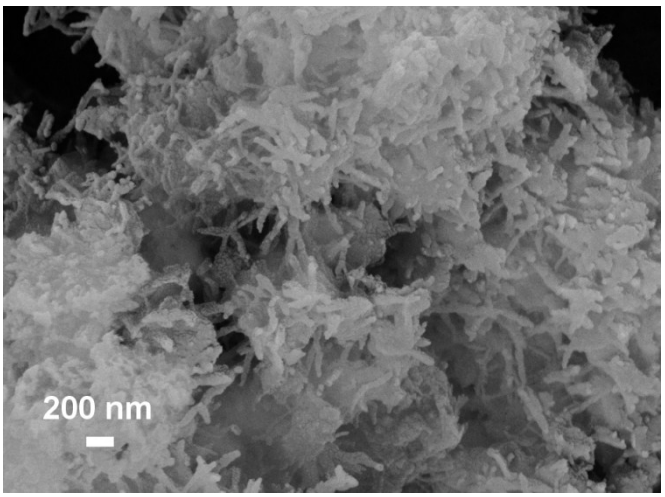

Figure S18. The SEM image of MoS_2-3%/TpPa-1-COF composite after photocatalysis.

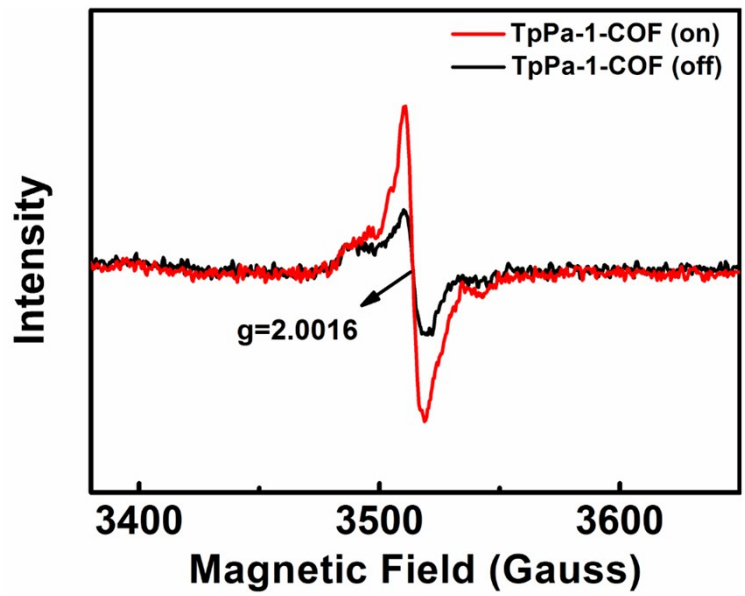

Figure S19. EPR spectra of TpPa-1-COF with light on and off.

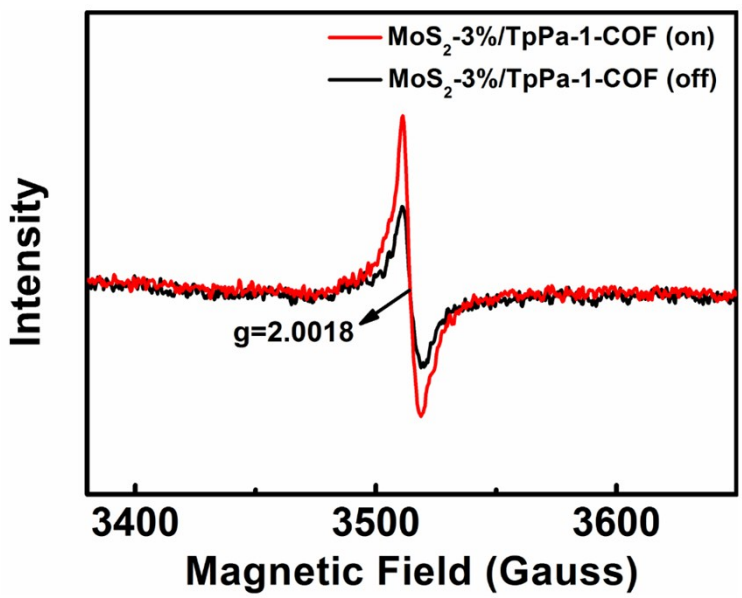

Figure S20. EPR spectra of MoS_2-3%/TpPa-1-COF with light on and off.

Table S1. Summary of H_2 evolution activity of photocatalyts.

Catalyst	Cocatalyst	Sacrificial agent	Illumination	Activity, $\mu mol \cdot g^{-1} \cdot h^{-1}$	AQE	Ref
TpPa-1-COF	MoS_2	Ascorbic acid	λ> 420 nm	5585	0.76%	This work
TpPa-1	Pt	Ascorbic acid	λ> 420 nm	5479	-	This work
TFPT-COF	Pt	Sodium ascorbate	λ> 420 nm	230	-	[1]
TFPT-COF	Pt	TEOA	λ> 420 nm	1970	2.2-3.9%	[2]
N_0-COF	Pt	TEOA	λ> 420 nm	23	0.001%	[2]
N_1-COF	Pt	TEOA	λ> 420 nm	90	0.077%	[2]
N_2-COF	Pt	TEOA	λ> 420 nm	438	0.19%	[2]
N_1-COF	Pt	TEOA	λ> 420 nm	1703	0.44%	[2]
PTP-COF	Pt	TEOA	λ> 420 nm	83.83	-	[3]
N_2-COF	Co-1[a]	TEOA	AM 1.5	782	0.16%	[4]
N_2-COF	Co-2[b]	TEOA	AM 1.5	414	-	[4]
N_1-COF	Co-1	TEOA	AM 1.5	100	-	[4]
N_3-COF	Co-1	TEOA	AM 1.5	163	-	[4]
COF-42	Co-1	TEOA	AM 1.5	233	-	[4]
g-C_3N_4 nanosheets	Pt	TEOA	λ> 420 nm	1860	3.75%	[5]
g-C_3N_4	MoS_2	Lactic acid	λ> 420 nm	1030	2.1%	[6]
S-doped mpg-CN	Pt	TEOA	λ> 420 nm	1360	5.8%	[7]
N-GQDs/g-C_3N_4	Pt	TEOA	λ> 420 nm	2180	5.25%	[8]
CdS	$Ni(OH)_2$	TEOA	λ> 420 nm	5084	28%	[9]
CdS	MoS_2	Lactic acid	λ> 420 nm	5530	79.7%	[10]
ZnS	CuS	Na_2S and Na_2SO_3	λ> 420 nm	4147	20%	[11]
$Zn_{0.8}Cd_{0.2}S$	RGO	Na_2S and Na_2SO_3	AM 1.5	1824	23.4%	[12]
Cu_2O	MoS_2	Methanol	λ> 420 nm	625	-	[13]
Mil-101/CdS	CDs	lactic acid	λ> 420 nm	488	-	[14]
g-C_3N_4	P	TEOA	λ> 420 nm	1596	3.56%	[15]
g-C_3N_4	CoP	TEOA	λ> 420 nm	1924	12.4%	[16]
g-C_3N_4/CdS	NiS	TEOA	λ> 420 nm	2563	-	[17]
CdS	Fe_2P	Ascorbic acid	λ> 420 nm	186	15%	[18]

g-C_3N_4	MoS_2	TEOA	λ> 400 nm	252	-	[19]
g-C_3N_4	WS_2	Methanol	λ> 420 nm	101	-	[20]
CdS/g-C_3N_4	NiS	TEOA	λ> 420 nm	2563	-	[21]
g-C_3N_4	$Ni_{12}P_5$	TEOA	λ> 420 nm	126.6	-	[22]

[b]Co-1: $[Co(dmgH)_2pyCl]$. [c]Co-2: $[Co(dmgBF_2)_2(OH_2)_2]$

Table S2. The fitting data of electrochemical impedance spectroscopy (EIS).

	TpPa-1-COF	MoS_2-3%/TpPa-1-COF
Rs	34.56	36.16
Rt	12666	5337
CPE-P	0.95	0.90
CPE-T	3.45E-5	4.39E-5

Reference

1. L. Stegbauer, K. Schwinghammer and B. V. Lotsch, *Chem. Sci.*, 2014, **5**, 2789-2793.
2. V. S. Vyas, F. Haase, L. Stegbauer, G. Savasci, F. Podjaski, C. Ochsenfeld and B. V. Lotsch, *Nat. Commun.*, 2015, **6**, 8508.
3. F. Haase, T. Banerjee, G. Savasci, C. Ochsenfeld and B. V. Lotsch, *Faraday Discuss.*, 2017, **201**, 247-264.
4. T. Banerjee, F. Haase, G. k. Savasci, K. Gottschling, C. Ochsenfeld and B. V. Lotsch, *J. Am. Chem. Soc.*, 2017, **139**, 16228-16234.
5. S. Yang, Y. Gong, J. Zhang, L. Zhan, L. Ma, Z. Fang, R. Vajtai, X. Wang and P. M. Ajayan, *Adv. Mater.*, 2013, **25**, 2452-2456.
6. Y. Hou, A. B. Laursen, J. Zhang, G. Zhang, Y. Zhu, X. Wang, S. Dahl and I. Chorkendorff, *Angew. Chem. Int. Ed*, 2013, **52**, 3621-3625.
7. J. Hong, X. Xia, Y. Wang and R. Xu, *J. Mater. Chem.*, 2012, **22**, 15006-15012.
8. J.-P. Zou, L.-C. Wang, J. Luo, Y.-C. Nie, Q.-J. Xing, X.-B. Luo, H.-M. Du, S.-L. Luo and S. L. Suib, *Appl. Catal. B*, 2016, **193**, 103-109.
9. J. Ran, J. Yu and M. Jaroniec, *Green Chem.*, 2011, **13**, 2708-2713.
10. K. Zhang, J. K. Kim, B. Park, S. F. Qia, B. Ji, X. W. Sheng, H. Zeng, H. Shin, S. H. Oh, C. L. Lee and J. H. Park, *Nano Lett.*, 2017, **17**, 6676-6683.
11. J. Zhang, J. Yu, Y. Zhang, Q. Li and J. R. Gong, *Nano Lett.*, 2011, **11**, 4774-4779.
12. J. Zhang, J. Yu, M. Jaroniec and J. R. Gong, *Nano Lett.*, 2012, **12**, 4584-4589.
13. Y.-F. Zhao, Z.-Y. Yang, Y.-X. Zhang, L. Jing, X. Guo, Z. Ke, P. Hu, G. Wang, Y.-M. Yan and K.-N. Sun, *J. Phys. Chem. C*, 2014, **118**, 14238-14245.
14. X. B. Meng, J. L. Sheng, H. L. Tang, X. J. Sun, H. Dong and F. M. Zhang, *Appl. Catal. B*, 2019, **244**, 340-346.
15. J. R. Ran, T. Y. Ma, G. P. Gao, X. W. Du and S. Z. Qiao, *Energy & Environmental Science*, 2015, **8**, 3708-3717.

16. C. M. Li, Y. H. Du, D. P. Wang, S. M. Yin, W. G. Tu, Z. Chen, M. Kraft, G. Chen and R. Xu, *Adv. Funct. Mater.*, 2017, **27**.
17. J. Yuan, J. Wen, Y. Zhong, X. Li, Y. Fang, S. Zhang and W. Liu, *J. Mater. Chem. A*, 2015, **3**, 18244-18255.
18. Z. J. Sun, H. L. Chen, Q. Huang and P. W. Du, *Catalysis Science & Technology*, 2015, **5**, 4964-4967.
19. H. Zhao, Y. Dong, P. Jiang, H. Miao, G. Wang and J. Zhang, *J. Mater. Chem. A*, 2015, **3**, 7375-7381.
20. M. S. Akple, J. Low, S. Wageh, A. A. Al-Ghamdi, J. Yu and J. Zhang, *Appl. Surf. Sci.*, 2015, **358**, 196-203.
21. J. Yuan, J. Wen, Y. Zhong, X. Li, Y. Fang, S. Zhang and W. Liu, *J. Mater. Chem. A*, 2015, **3**, 18244-18255.
22. J. Wen, J. Xie, R. Shen, X. Li, X. Luo, H. Zhang, A. Zhang and G. Bi, *Dalton Trans.*, 2017, **46**, 1794-1802.